ACS Biomaterials SCIENCE & ENGINEERING
Cite This: ACS Biomater. Sci. Eng. 2019, 5, 6436−6445
Article
pubs.acs.org/journal/abseba

Effect of Topographical Steps on the Surface Motility of the Bacterium *Pseudomonas aeruginosa*

Yow-Ren Chang,[†] Eric R. Weeks,[‡] Daniel Barton,[§] Jure Dobnikar,[§,∥,⊥] and William A. Ducker*[,†]

[†]Department of Chemical Engineering and Center for Soft Matter and Biological Physics, Virginia Tech, Blacksburg, Virginia 24061, United States

[‡]Department of Physics, Emory University, Atlanta, Georgia 30322, United States

[§]Institute of Physics, Chinese Academy of Sciences, Beijing 100190, P. R. China

[∥]Songshan Lake Materials Laboratory, Dongguan, Guangdong 523808, P. R. China

[⊥]Department of Chemistry, University of Cambridge, Lensfield Road, CB21EW Cambridge, U.K.

Supporting Information

ABSTRACT: Bacteria traverse surfaces as part of colonizing solids, and it is of interest to hinder this motion to potentially thwart infections in humans. Here, we demonstrate that topographical steps hinder the ability of *Pseudomonas aeruginosa* PAO1 (*P. aeruginosa*) to traverse a solid−liquid interface. Using time-lapse fluorescence microscopy and image analysis, we analyzed the motion of *P. aeruginosa* that were challenged with steps ranging in height from 0.4 to 9.0 μm. Bacterial trajectories are sensitive to the height of the step, the curvature of the step face, and the direction of their motion relative to gravity. When the step height is $\geq$0.9 μm, which is similar to the cell diameter, there is a reduced probability of the cell crossing the step. For those bacteria that do cross a step, there is a time penalty for crossing steps of height 2−3 μm; this height is similar to the length of the bacterium. For higher steps, the bacteria reorient their cell body while traversing the step riser. Our findings elucidate how topography influences the motion of bacteria and informs strategies for hindering bacterial motion at surfaces.

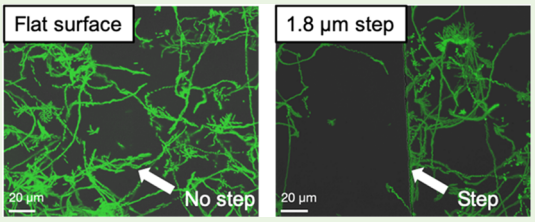

KEYWORDS: *Pseudomonas aeruginosa, twitching motility, surface topography, biofilms*

INTRODUCTION

Pseudomonas aeruginosa (*P. aeruginosa*) is an opportunistic human pathogen known to form biofilms, which are communities of bacteria encased in an extracellular matrix at an interface.[1,2] Biofilms are particularly devastating in a hospital setting as bacteria can colonize medical devices and cause infections in patients that are difficult to treat.[3] Therefore, researchers have been motivated to develop methods of preventing bacterial biofilm growth on surfaces. Several methods have been proposed in the literature such as the use of liquid-infused surfaces,[4,5] contact killing surfaces,[6,7] dynamic substrates,[8−10] and the use of microtopographical features.[11−13] Our group has recently demonstrated that microparticle arrays known as colloidal crystals with particle diameters on the μm scale can hinder biofilm growth and that the effect of topography is additive to the effect of an antimicrobial surface film or a solution antibiotic treatment.[14−16]

While the effects of surface topography on bacterial biofilm formation have been studied, the mechanism(s) of action remains poorly understood and limits our ability to design better antibiofilm topographical surfaces. There are several stages in the biofilm formation process,[17] and the behavior of bacteria in each stage could be impacted by surface topography. Recent work has examined how the probability of attachment is affected by topography.[18,19] Here, we focus on how the topography impacts the surface motility of a particular bacterium, *P. aeruginosa*. *P. aeruginosa* is a rod-shaped bacterium, for which surface twitching motility is important for biofilm formation.[20,21] Twitching motility is achieved by the extension and retraction of several μm long polymeric appendages known as type IV pili.[22,23] The dynamics of type IV pili leads to a wealth of motility behaviors[24−28] that may assist *P. aeruginosa* with the navigation of a surface, and the pili may even act as sensors for biofilm formation.[29] As we demonstrate, the motion of surface motile bacteria is impacted by surface topography; therefore, it is possible that the topography will also impact biofilm formation.

Meel et al. first investigated the effect of micrometer-scale grooves of 0.6 and 1 μm heights on the motility of *Neisseria gonorrhoeae* and *Myxococcus xanthus*, both of which exhibit surface motility via type IV pili.[30] They found that both organisms appeared to preferentially move within the grooves and that it was more difficult for them to cross taller (1 μm) grooves than shorter (0.6 μm) grooves.[30] We previously investigated the effect of periodic, close-packed, half-sphere arrays on the surface motility of *P. aeruginosa* and found that there was a threshold diameter between 1 and 2 μm where the

Received: May 22, 2019
Accepted: October 28, 2019
Published: October 28, 2019

DOI: 10.1021/acsbiomaterials.9b00729
ACS Biomater. Sci. Eng. 2019, 5, 6436−6445

motion was hindered.[31] This is similar to the dimensions of the bacterium. We also found that the bacteria preferentially moved in the grooves between particle caps and that bacteria were rarely found on top of the spherical caps.[31] Importantly, the half-sphere texture reduces the average displacement of the bacteria, thereby demonstrating that topography can inhibit motility. Other recent work has demonstrated that nanopillars also hinder the motion of bacteria.[32] The macroscopic migration of *Escherichia coli* cells has also been examined on textured surfaces.[33]

Here, we explore the effect of topographic steps on surface motility under a negligible flow rate (surface shear stress ~4×10^{-4} Pa) so that we can isolate the effect of topography alone. The low applied flow rate is to provide nutrients and remove waste. Previous work has shown that much higher shear stresses ($100-10^5$ times larger than in our work) cause bacteria to move upstream.[27] Low or zero flow rate is relevant to many biomaterials, e.g., prostheses or catheters (e.g., central venous catheters,[34] PICC lines,[35] and PEG tubing[36,37]) where there is often zero flow for many hours. Both hydrodynamic and gravitational forces are much smaller ($10^{-14}-10^{-15}$ N) than the forces that the pili can exert (typically 10^{-10} N).[38]

In the current work, we study bacterial interactions with widely spaced, vertical steps to understand in more detail how a motile bacterium copes with a single topographic feature. We envision that to cross over that step, a bacterium must be able to attach a pilus over a step and pull its body in a direction that contributes to the overall motion. We hypothesize that there is a minimum step height required to measurably hinder the motion of *P. aeruginosa*. To test this, we fabricated topographical steps (see Figure 1A) of various heights between 0.4 and 9 μm, which spans the dimensions of the bacteria (diameter ~1 μm, length 2−3 μm) and the pili (several μm).[22] The bacteria were viewed through the topographic sample using an upright microscope such that gravity points from the solid to the liquid. Thus, we refer to the part of the step that is higher with respect to gravity as the "high" side and the other plane as the "low" side (see Figure 1). We recorded the motion of constitutively fluorescent *P. aeruginosa* cells on the interface between the stepped topography and the liquid environment at 37 °C using time-lapse fluorescence microscopy (Figure 1B). With image analysis and particle tracking methods, we analyzed the trajectories of single *P. aeruginosa* cells in relation to the topographical step. We also tested the hypothesis that bacteria will traverse a topographical step with or against gravity (Figure 1C) with the same probability. Neglecting the weak force of gravity, these paths are the same, except in the opposite order. Furthermore, we analyzed the modes of motion of single *P. aeruginosa* while crossing a step.

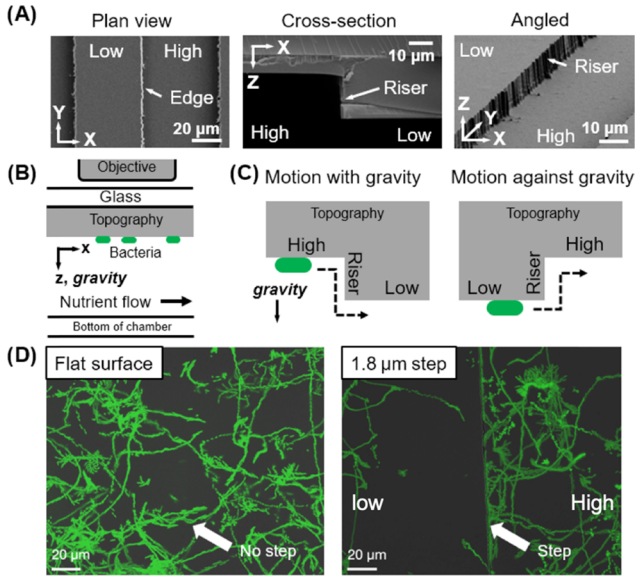

Figure 1. (A) Scanning electron microscope (SEM) images of a fabricated topographical step: taken from a direction perpendicular to the plane (plan view), parallel to the plane (cross-sectional view), and at an intermediate angle (angled view). (B) Schematic of the experimental setup. Note that the sample is at the top of the fluid cell so that the gravity points away from the sample, in the direction of positive *Z*. (C) Schematic to describe the terms used to refer to the motion of a bacterium crossing a step. We refer to the part of the solid that is parallel to the gravity as the riser. The dashed arrow in the left sketch shows two hypothetical turns: an "inside turn" followed by an "outside turn;" the order is reversed for the motion in the right sketch. (D) maximum intensity image showing the positions visited by the bacteria over 100 min on a flat surface and when a single 1.8 μm step runs from the top to bottom of the image in the middle. The fluid flow direction is from the left to right.

MATERIALS AND METHODS

Bacterial Growth. A constitutively fluorescent strain of *Pseudomonas aeruginosa* PAO1 that produces the fluorescence protein *tdTomato* was used for all studies (a gift from Prof. Joe Harrison, Univ. of Calgary). All growth mediums were supplemented with 30 μg/mL gentamycin. Tryptic soy agar plates were streaked with frozen stock and incubated at 37 °C overnight. A 250 mL baffled flask with a foam stopper and 50 mL of tryptic soy broth (TSB) were inoculated with a single colony from the agar plate. This culture was grown overnight at 300 rpm and 37 °C. A subculture was started by inoculating 50 mL of TSB with 50 μL of the overnight culture and incubating in a baffled flask at 300 rpm and 37 °C for 4 h to reach the early exponential growth phase, as monitored by optical density measurements. The suspension was diluted to OD_{600} 0.01 and then immediately used for flow chamber experiments.

Fabrication of Topographical Step Features. Silicon wafer masters of topographical steps were fabricated using a standard deep-reactive ion etching process (DRIE) at the UNC CHANL microfabrication laboratory. Patterns were developed using photolithography on a Si wafer (⟨100⟩ N-type 100 mm diameter wafer purchased from University Wafer). The wafer was initially coated with a primer using spin-coating (MicroChem MCC Primer 80/20) at 3000 rpm for 30 s to improve adhesion between the photoresist and the wafer during the etching process. A positive photoresist (MicroChem S1813) was then spin-coated onto the surface at 3000 rpm for 30 s and subsequently baked for 1 min at 95 °C. The wafer was then selectively exposed via the photomask to UV radiation using a dose of ~10 mW/cm^2 for 8 s and then developed in MF1319 for 60 s to expose the pattern for the steps on Si. Etching of the patterned Si wafer was performed using DRIE at 20 °C with alternating pulses of SF_6 at 200 cm^3/min for 3 s (etching) and C_4F_8 at 100 cm^3/min for 1.5 s (passivation) for a total etch rate of 1 μm/min. Finally, the remaining photoresist was stripped from the Si wafer using O_2 plasma in the DRIE to expose the etched steps in silicon.

The test samples for the bacteria experiments were Norland Optical Adhesive replicates of the silicon masters. To fabricate these replicates, we made a silicone mold that was a negative of the silicon pattern. The silicon wafers with the step topography were first oxygen-plasma-treated (Harrick Plasma) and then coated with nonafluorohexyltrichlorosilane (Gelest) via vapor deposition to act as an antiadhesion layer. Polydimethylsiloxane (PDMS) negative molds were fabricated by pouring mixed and degassed Sylgard 184 (Dow Corning, 10:1 base to curing agent) onto the wafers and curing the PDMS at 60 °C overnight. Positive replicates were then fabricated in Norland Optical Adhesive 81 (NOA, Norland Products) by spin-coating NOA onto cleaned cover

DOI: 10.1021/acsbiomaterials.9b00729
ACS Biomater. Sci. Eng. 2019, 5, 6436−6445

glass slides at 3000 rpm for 10 s, pressing the PDMS mold, and then UV-curing the NOA. The curing process took place in two stages, an initial cure at 400 mW from 6 inches away for 120 s (Omnicure Series 1000, Excelitas Technologies) and a final cure in a UV/ozone cleaner (Bioforce Nanosciences) for 10 min. We refer to the final step structure as the "sample". Figure 1A–C shows the scanning electron microscopy (SEM) images of the positive NOA steps along with the coordinate system we use in this work. The top-down view of the steps is the $X-Y$ plane (Figure 1A), and a cross-sectional view of the step (Figure 1B) shows the $X-Z$ plane. Note that the riser of the step is not perfectly planar; it has a curvature in the Y direction but not the Z direction (Figure 1C). Atomic force microscopy images showed that the flat sample had an RMS roughness of ∼2 nm over an area of 1 μm × 1 μm, much less than any of the step heights. We made two different sample types: one with steps that were 200 μm apart and the other with steps 50 μm apart. Motility experiments were performed using both spacings and, unless otherwise specified, the results of both experiments were combined. Table 1 shows the measured step heights of both sample types determined from cross-sectional SEM images. In the remainder of the text, we refer to the step heights by their nominal values: 0.4, 0.9, 1.8, 3, 5, and 9 μm. The flow chamber was finally created by gluing with PDMS a topographic sample on its glass coverslip to a flow chamber and curing the PDMS at 60 °C. Steps were always arranged such that the edge ran perpendicular to the direction of flow.

Table 1. Measured Step Heights from Cross-Sectional SEM Images[a]

nominal height (μm)	measured height (50 μm spacing) (μm)	measured height (200 μm spacing) (μm)
0.4	0.4	0.4
0.9	0.9	0.9
1.8	1.8	1.8
3	3.1	2.7
5	5.1	5.0
9	9.1	9.4

[a]Images are shown in Figure S1. The measurement uncertainty in step height is ±0.2 μm.

Motility Experiments. Flow chamber experiments were performed as previously described.[31] The flow setup consisted of a medium bottle, a peristaltic pump, a bubble trap, the flow chamber, and a waste bottle. The channel is 4 mm wide, 1 mm deep, and 50 mm long. The flow setup was autoclaved prior to use and then placed in a custom-built microscope enclosure held at 37 °C. The medium used in flow experiments was 100% (30 g/L) TSB and was pumped at ∼4 mL/h. The Reynolds number (Re) at this flow rate was calculated to be ∼0.004. Prior to imaging, the flow was stopped and 150 μL of bacterial suspension (see the section on bacterial growth) was injected into each channel of the flow chamber to inoculate the surface. Bacteria were allowed to attach to the surface for 10 min under no-flow conditions. The flow of the medium was resumed to flush out nonattached bacteria for 10 min; at the flow rate used, this exchanged the volume of the flow chamber approximately 3 times. After flushing, the flow of the medium continued to provide nutrients and remove waste, and the motion of bacteria at the solid–liquid interface was recorded.

We imaged the surface motility of *P. aeruginosa* using a motorized Zeiss Imager.M2 upright fluorescent microscope equipped with a 63 × 1.4 numerical aperture, oil immersion lens. Brightfield images were collected to visualize the topographical step, and fluorescence images (excitation: 545/25 nm, beam splitter: 570 nm, emission: 605/70 nm) were collected to visualize the bacteria. Images were captured in grayscale and colored green. Time-lapse movies were collected at a rate of one image every 30 s for 2 h, starting ∼20 min after the inoculum period (10 min for attachment and then 10 min to flush), and ∼200 bacteria were tracked in each experiment. Lamp intensities and exposures were optimized to prevent phototoxicity; we previously demonstrated that the surface motility of *P. aeruginosa* under these imaging conditions is neither affected by fluorescence imaging nor does the motility of the fluorescent strain differ from the wild type.[31] Since bacteria could be located at different focal planes, low steps (0.4–3 μm) were imaged twice, with one z-slice focused on the low plane and one on the high plane. The high steps, 5 and 9 μm, were imaged with 3 and 4 z-slices, respectively.

Image and Data Analyses. *Tracking.* All image and data analyses were performed using MATLAB (MathWorks). For image analysis, fluorescence images were used to identify and track bacteria and brightfield images were used to detect the steps. Fluorescence images were collapsed in the z direction to yield a 2-D image that showed bacteria on both the high and low sides of the step. Bacteria were tracked using standard particle tracking methods.[39] The length of bacteria was measured by binarizing fluorescent images and measuring the long axis of an ellipse with the equivalent second moment using built-in MATLAB functions.

Statistics. For the purposes of statistical analyses, we consider an experimental replicate to be all of the results obtained from a fresh culture of bacteria with a fresh solid sample on a new day. The individual bacteria were not considered to be replicates. The standard error, derived from the number of replicate movies, is indicated by error bars or shaded regions in the figures. We repeated experiments with each step height at least 3 times. Across all step heights and replicates, we identified ∼700 crossing events over ∼10 000 frames (45 movies total). Statistical testing was performed with t-tests or the analysis of variance (ANOVA) followed by a multiple comparison test when appropriate. In general, we considered differences with p-values less than 0.05 to be significant.

RESULTS

Effect of Flow on the Flat Surface Is Insignificant. All results are for cells that were allowed to adsorb for approximately 20 min before imaging was commenced. At this point, most of the cells are exhibiting surface motility and there are no clusters of cells at the solid–liquid interface. We designed our experiments such that the very slow fluid flow should not influence the motion of bacteria. To verify this, we calculated the mean displacement of bacteria in a given time interval on a flat surface in the X and Y directions, $\langle d_x \rangle$ and $\langle d_y \rangle$. We find that $\langle d_x \rangle = -0.06 \pm 0.07$ μm in 5 min and $\langle d_y \rangle = -0.16 \pm 0.12$ μm in 5 min, showing that the presence of flow (in the $+X$ direction) does not bias the motion of bacteria. Furthermore, we find that the mean absolute displacements in X and Y, $\langle |d_x| \rangle$ and $\langle |d_y| \rangle$, are not statistically different from each other (t-test, p-value = 0.67), indicating that bacterial motion is isotropic.

Steps Reduce the Crossing Probability of Bacteria. Fluorescence images of bacteria suggested that bacterial trajectories on the solid–liquid interface are affected by the presence of a step (see Figure 1D). The first metric that we used to quantify the effect on trajectories was the probability of crossing a step. To define a crossing, we needed a starting line on one side of the step and a finish line on the other side, and we defined a step zone between these lines. The inspection of brightfield images of the step showed that the edge is not exactly straight; thus, we fitted the edge with a line and defined a step zone that extended 1.8 μm on each side of the step (see the inset of Figure 2A). We defined the crossing probability as

$$\frac{\text{number of bacteria that traversed entire width of step zone}}{\text{number of bacteria that were ever in the step zone}} \quad (1)$$

Figure 2A shows that the measured crossing probability is dramatically reduced from 0.68 ± 0.03 on a flat surface to ≈0.2 on steps taller than 0.9 μm (Figure 2A). For a flat surface, we drew artificial steps and noted that the crossing probability is not 1 because bacterial motion is not ballistic. We analyzed the

DOI: 10.1021/acsbiomaterials.9b00729
ACS Biomater. Sci. Eng. 2019, 5, 6436–6445

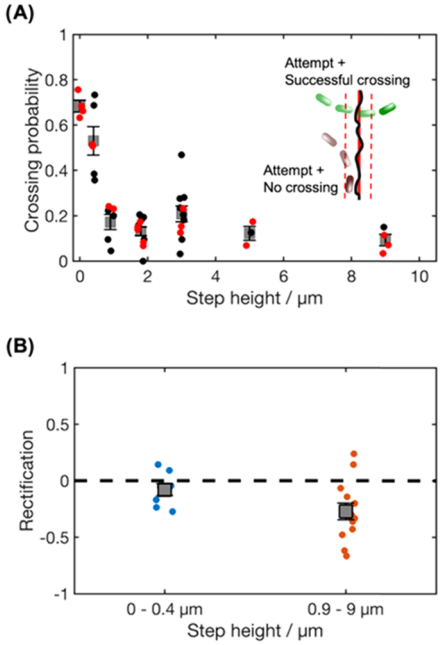

Figure 2. (A) Probability of *P. aeruginosa* crossing a step. Circles represent individual experimental replicates. Black indicates experiments performed with a single topographical step in a field of view; red indicates experiments with multiple steps in a field of view. The average for each step height is shown in square markers, and the error bars are the standard error. We identified 736 crossing events across all experiments. Statistical comparisons: 0 vs 0.4 μm, $p = 0.20$, $p \ll 0.001$ for each pair-wise comparison between 0 and 0.9−9 μm and between 0.4 and 0.9−9 μm, $p \gg 0.1$ for each pair-wise comparison between step heights in the range 0.9 −9 μm. Inset: schematic showing the step and both successful and unsuccessful attempts to cross. The black line represents the step in the image, the red line is the fitted line, and the dotted red lines show the limits of the step zone. (B) Rectification of motion of *P. aeruginosa* crossing a topographical step. We did not include data from steps where the total number of crossings was less than 10. Circular markers show data for a single experiment, square markers show the average, and the error bars are the standard error. The step heights are grouped into two groups: 0−0.4 and 0.9−9 μm heights. The negative rectification for 0.9−9 μm heights shows a bias for motion against the direction of gravity.

results by performing an ANOVA followed by a Tukey−Kramer multiple comparison test and found that the crossing probabilities for 0 and 0.4 μm were both different from the crossing probabilities for all steps taller than 0.9 μm ($p \ll 0.001$ for each pair-wise comparison between 0 and 0.9−9 μm and between 0.4 and 0.9−9 μm). We hypothesized that there might be an intermediate step height, of the order of the length of the bacteria (≈3 μm), that was more difficult to cross; however, we did not find a statistically significant difference in the crossing probability for any pairs of heights in the range 0.9−9 μm.

We then tested whether the crossing probability was affected by either (1) the direction of gravity or (2) the direction of flow relative to the direction of motion. An ANOVA showed that the direction of motion relative to gravity was significant ($p = 0.017$), but the flow direction was not ($p = 0.59$), nor was the interaction between factors ($p = 0.34$) (see the Supporting Information Section 1, Figure S2).

Having demonstrated that the flow was unimportant under the conditions studied, we further examined the motion up and down the steps with the concept of rectification, defined as

$$\frac{\text{number of crossings with gravity} - \text{number of crossings against gravity}}{\text{total number of crossings}} \quad (2)$$

The average rectification for 0−0.4 μm steps was −0.08 ± 0.05 indicating no preference for or against gravity, whereas for step heights in the range of 0.9−9 μm, the average rectification was −0.27 ± 0.07 (Figure 2B). Thus, we have resolved a preference for travel against gravity ($p = 0.003$ for comparison between 0.9−9 μm steps and no step).

Bacteria Are More Likely To Be Found Near a Step Edge. We examined the positional distribution of bacteria on the high and low sides of the step by measuring the perpendicular distance between a bacterium and the step (see the inset in Figure 3). Figure 3 plots a distribution of these positions. Flat surfaces with fictional step edges were used as zero step height controls, for which we found the time-average probability to be spatially homogeneous (gray data in Figure 3). The data were similar to the 0.4 μm step heights.

For all steps of greater height, there was an increased probability of finding bacteria at or near the step edge (<5 μm

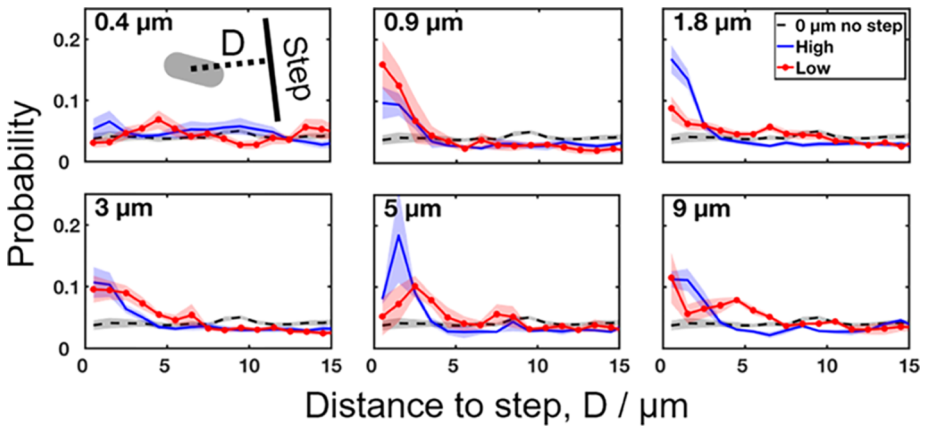

Figure 3. Probability distribution of the distance to a step. High means that the bacterium is on the high part of the step, and low means the bacterium is on the low side of the step (see Figure 1C). For each step height, we compare to results for a flat surface, which is labeled in the legend as 0 μm no step. The distance is measured from a line that is fitted to the image of the step. Bacteria are more likely to be found near steps when the step height is greater than about 0.9 μm. Only data from samples with a 50 μm spacing between steps were used in this analysis. Data include a total of ∼400 000 measurements. The average probability at a certain distance is drawn as a solid line, and the standard error is shown as a shaded region around the average.

DOI: 10.1021/acsbiomaterials.9b00729
ACS Biomater. Sci. Eng. 2019, 5, 6436−6445

away; see Figure 3). Previous work has shown that bacteria can be aligned with topographic features.[15,40,41] Interestingly, here, we have shown that the bacteria have a higher probability of being on both sides of a step: where it is near a wall (concave to liquid in the $X-Z$ direction) or when on the low side, near a void (convex to the liquid in the $X-Z$ direction). Overall the high side of the step does not have a consistently lower or higher density than the low side of the step. To summarize, not only is crossing a step reduced (Figure 2A) but also this leads to an accumulation of bacteria near the step, rather than "reflecting" them away from the step.

Motion toward a Topographical Step Is Reduced Near the Step. We next investigated how bacteria move near the step edge. We calculated the displacement vector of each bacterium over a 5 min time interval, Δr, as a function of the perpendicular distance to a step edge at the start of the measurement period. We decomposed Δr into components that were parallel ($\Delta r_{\parallel}$) and perpendicular ($\Delta r_{\perp}$) to the step, as shown in the inset of Figure 4. The average value of $|\Delta r_{\parallel}|$ is independent of the step

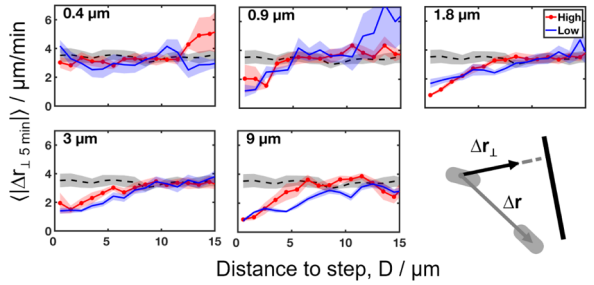

Figure 4. Average displacement of cells in 5 min as a function of the initial distance from the step. The distance was measured to a line fitted to the brightfield image of the step. The perpendicular component of displacement (as shown in the schematic) is plotted, and each panel is labeled by the step height. Data from samples with a 50 μm spacing between steps were used. Lines are the average, and shaded regions indicate the standard error. A total of ~200 000 displacements were measured. Data for a 5 μm step height are shown in Figure S4.

height and proximity of the bacterium to the step (Figure S3). For perpendicular motion, we only considered displacements toward a step edge. Figure 4 plots the average value, $\langle|\Delta r_{\perp}|\rangle$, as a function of the starting distance to the step, D, for different step heights. For 0.9−9 μm steps, $\langle|\Delta r_{\perp}|\rangle$ gradually decreases by half for those starting within 10 μm of step edge. Since type IV pili are several μm in length, this could be the range in which type IV pili are sensing the step. These data suggests that motion of bacteria toward a topographical step is hindered if the step is of sufficient height (> 0.4 μm).

Steps Are Not Simply Extra Distance for a Bacterium To Travel. When a bacterium crosses a step, it must also travel over an extra distance to traverse the height of the step. In the simplest model, the extra distance could be modeled as an extra section of flat terrain (see Figure 5A), and turning the corners (Figure 1C) would not require any extra time or otherwise affect the trajectory. Because motion is not ballistic, the extra distance would not simply add a proportional amount of time; in fact, we have shown previously that the mean-squared displacement is proportional to $(\Delta t)^{1.5}$, where t is the time.[31] We examined this simple model by comparing the time for a bacterium to cross a real step (Figure 5A, left), t, to the time to cross a section of a flat surface of the equivalent distance as a step (Figure 5A, right), t_{eq}. The data in Figure 5B suggest that for both 1.8 and 3 μm steps

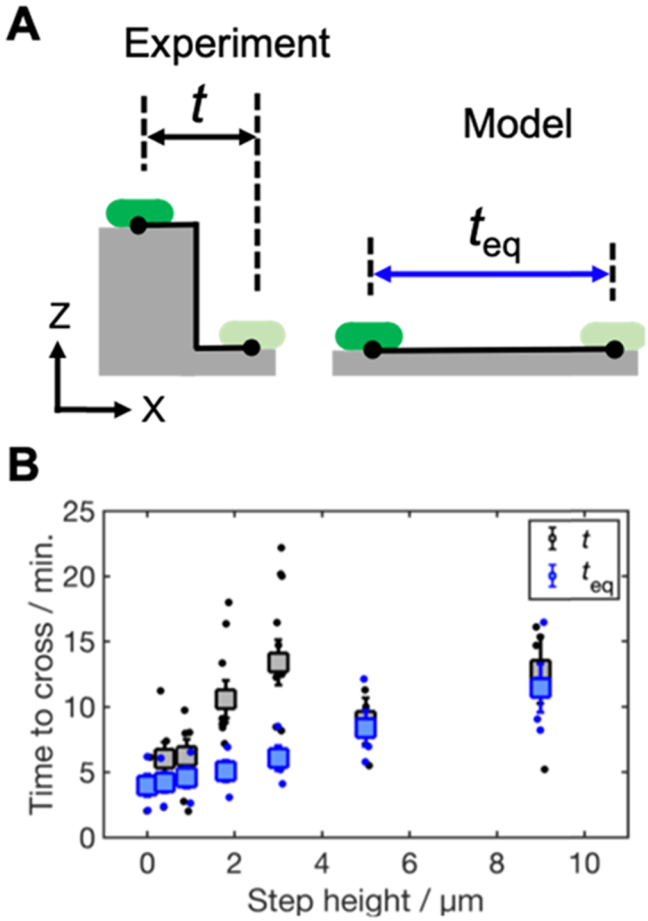

Figure 5. (A) Bacterium takes a time, t, to traverse the step zone. In the model, a bacterium on a flat sample takes a time, t_{eq}, to cross a step zone that is widened by a length equal to the height of the step. (B) Time for *P. aeruginosa* to traverse a topographical step as a function of the step height. The arithmetic mean time to cross of individual replicates is plotted as circular markers, and the grand average (average of the averages) is plotted as square markers. The error bars indicate the standard error. The time to cross a real step, t, is compared to the time to cross a flat surface with a step zone widened by a length equal to the height of the step, t_{eq}. Note that markers for the grand average t and t_{eq} for the flat (0 μm) surface overlap each other. We identified 736 crossing events across all experiments. A two-factor ANOVA with a step height (p = 0.003) and experiment versus model (p = 0.008) demonstrated that, in general, steps are not just extra distance to travel.

there is an additional time, but for both higher and lower steps, the additional time is difficult to resolve. Of course, for the higher steps, many bacteria fail to cross at all (Figure 2A); the data of Figure 5B are only for those bacteria that succeed in crossing a step.

To enable multiple comparison tests, we calculated the difference between the experimental and model times, $\Delta t_{cross} = t - t_{eq}$. We found that Δt_{cross} was significantly different from zero only for 1.8 and 3 μm steps (p = 0.04 for 0 vs 1.8 μm and p = 0.006 for 0 vs 3 μm) and not for the higher steps. Since the p-value for the comparison between 0 and 1.8 μm was close to the value that we set for significance, we performed three additional entirely independent experiments on only the 1.8 μm steps. The p-value for new experiments yielded p = 0.15; so, we are not in a position to make a conclusion that the 1.8 μm step, in particular, requires additional time beyond the time to traverse the distance of the riser. However, we do conclude that the bacteria took

DOI: 10.1021/acsbiomaterials.9b00729
ACS Biomater. Sci. Eng. 2019, 5, 6436−6445

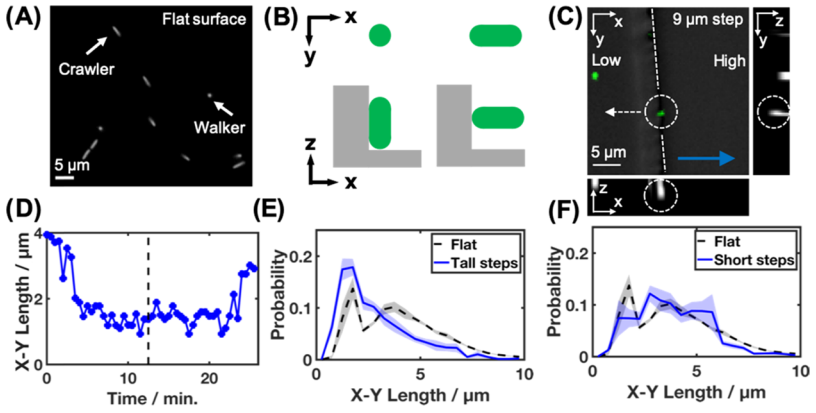

Figure 6. (A) Fluorescence image of several *P. aeruginosa* cells of different aspect ratios on a flat surface. The image shows the cross section in the $X-Y$ plane. The large aspect ratio is the crawling mode and the low aspect ratio is the walking mode. (B) Schematic of the bacterium (green) on a riser as seen in the $X-Y$ plane and from the side ($X-Z$ plane). (C) Fluorescence image (green) of *P. aeruginosa* on a 9 μm topographical step (gray) shown for the $X-Y$, $X-Z$, and $Y-Z$ planes. The same bacterium is circled on the three images. This bacterium appears circular in the $X-Y$ image but is more elongated in the $X-Z$, and $Y-Z$ planes. The dashed white line shows the position of the step; the white dashed arrow shows the direction of the bacterial motion; the blue arrow shows the direction of the flow. The Z scale has been rescaled in the $X-Z$ and $Y-Z$ images. (D) Time course of the measured $X-Y$ length of the bacterium shown in (C). The dashed line in (D) indicates the time of the image shown iin C. The dashed line in D indicates the time of the image shown in C. Prior to being on the riser, the bacterium is crawling. The bacterium then reorients to crawl on the riser and then reorients again as it travels on the plane on the far side of the step. (E) Probability distribution of the $X-Y$ lengths of bacteria in the step zone on tall topographical steps (step height 3−9 μm) compared to the distribution on a flat topography. On the flat, the distribution is bimodal, representing a majority of crawlers (large $X-Y$ length) and a minority of walkers (short $X-Y$). On the step, there is a large peak for small $X-Y$ lengths, which we interpret as a majority of crawlers. (F) Probability distribution of the measured $X-Y$ lengths of *P. aeruginosa* while crossing small topographical steps (0.4−1.8 μm). For (E) and (F), the average is plotted as solid lines, and shaded regions indicate the standard error.

extra time, about 2.5× as long, to cross the 3 μm step. We explore the implications of this finding further in the Discussion section. On higher steps (5 and 9 μm), the main effect of the step appears to be the extra distance required for travel; the extra time to turn the corners was small.

Bacteria Crossing Tall Steps Predominately Do So in the Crawling Mode. We investigated the mode in which bacteria crawled up a step. It is well known that on a flat surface, *P. aeruginosa* can adopt different modes of surface motility. The bacteria can "crawl", where the long axis of the body is parallel to a surface, or "walk", where the long axis is perpendicular or angled to the surface.[42] We cannot directly measure the tilt angle, but the projection onto the $X-Y$ plane can be used as a proxy for it: in an $X-Y$ image, crawlers on the high or low plane appear as rods and walkers appear as circles (Figure 6A). We also infer the motility mode on the riser by measuring the $X-Y$ length, but on the riser, a short $X-Y$ length indicates a crawler (Figure 6B). Figure 6C shows the data for a bacterium on the riser: the bacterium has a small $X-Y$ length and therefore is crawling down the riser. Figure 6D shows a time course of the same bacterium. The time course shows two changes in the $X-Y$ length, demonstrating that the bacterium started as a crawler on the flat, then rotated once so that it could maintain the crawling model on the riser, and then rotated again on the flat after it passed the step. That was data for only one bacterium, but Figure 6E compares the measured probability distribution of the projected bacterial length on a flat surface to the probability of tall steps (3−9 μm) while crossing. On the flat, there is a bimodal distribution with most of the probability in the long $X-Y$ (crawling) mode, as described previously.[42] On the tall steps, there is a much greater probability for short $X-Y$ lengths, which corresponds to the crawling mode on the vertical step risers. There is a broad tail in the distribution for long lengths, i.e., the walking mode on the steps. Thus, the bacteria primarily crawl up the tall steps. On the short steps (0.4−1.8 μm), it is difficult to resolve a difference from the probability distribution on the flat. It is also difficult to define a walker and crawler because the bacterial length is similar to the height of the step.

Local $X-Y$ Step Curvature Influences Bacterial Passage over the Step. In the analysis so far, we have ignored the fact that the risers in our samples have curvature in the $X-Y$ plane with the radius of the same order as the bacteria (~1 μm). We hypothesize here that the bacteria that do cross are more likely to do so when the step topography is concave toward them (assigned negative; see Figure 7A). Regions of a negative curvature would give a greater cone angle where the pili could strike the riser (see Figure 7A). This hypothesis was inspired by the author's experience that we find it is easier to climb rock faces that have a negative curvature on our human scale than to climb rock faces with a positive curvature.

To test this hypothesis, we first characterized the local curvature by fitting a curved line in the $X-Y$ plane to the image of the step edge and then characterized the local radius of curvature at each point on this curve (see Figure 7B and the Supporting Information Section 2 and Figure S5 for further details). The distribution plotted in Figure 7C shows that the positive and negative curvatures are equally likely in each curvature range, and there are many radii in the range of 0−2 μm. We compared this distribution to the distribution of local curvature at the bacterial crossing points. For each bacterium in each frame, we fitted an ellipse to the image of the bacterium and measured the overlap of the ellipse and the curved step edge line. Any point of overlap was considered to be an interaction (Figure 7C inset), and the curvature at the interaction point was included in the distribution of interactions. Figure 7C compares the distribution of step curvature with the distribution of interaction curvatures. Comparing the distribution of step curvature to the distribution of interaction curvature, there is an excess of interactions on the small negative curvature. This

DOI: 10.1021/acsbiomaterials.9b00729
ACS Biomater. Sci. Eng. 2019, 5, 6436−6445

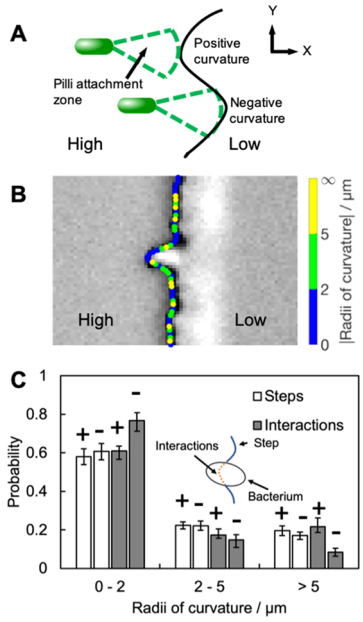

Figure 7. (A) Schematic showing the curvature of the step. A possible zone of pilus attachment points has a greater overlap on the concave (negative curvature) region of the step. (B) Sample results of the measurement of the radius of curvature. The color indicates the radius of curvature. (C) Probability distributions of the curvature. Step curvature is the distribution of the curvature on the steps. Interaction curvature is the distribution of curvatures where the bacteria interacted with the steps (see the inset). Crossing bacteria were more likely to interact with the concave regions of the step. Error bars indicated the standard error, and signs above the columns indicated a positive or negative curvature.

suggests that the bacteria are more likely to cross a step at the locally concave curvature sites.

DISCUSSION

Increasing the Impediment to Motility. We investigated how the opportunistic human pathogen *P. aeruginosa* navigates topographical steps of heights 0.4–9 μm. Our data demonstrate that steps of 0.9 μm or taller significantly hinder the ability of the bacteria to traverse a solid–liquid interface. Since surface topography has been shown to be important for bacterial biofilm formation, our results could have implications for the design of topographical surfaces for biofilm prevention or help elucidate the mechanisms of topography in slowing down the biofilm growth. First, the demonstrated reduction in movement by the steps may hinder the bacteria from finding each other and therefore hinder the biofilm growth. Second, the reduction in movement may slow the spread of the bacteria from one point to another. For example, it might potentially slow the progression of the bacteria up catheters and into patients.

To increase the impediment to the bacteria, we fabricated samples with a greater density of steps and steps running in both X and Y directions: a 50 × 50 μm^2 raised square patterns (checkerboard) of a 2 μm height. Figure 8A shows a maximum intensity image from a 2 h time-lapse movie of *P. aeruginosa* on this checkboard. The image indicates that trails of *P. aeruginosa* interact with the walls of the checkerboard pattern. We tracked the bacteria, quantified the average speed on a 2 μm checkerboard pattern, and compared that to the average speed of the bacteria on a flat surface. We found that on the 2 μm checkerboard pattern, the average displacement in 5 min was 4.7

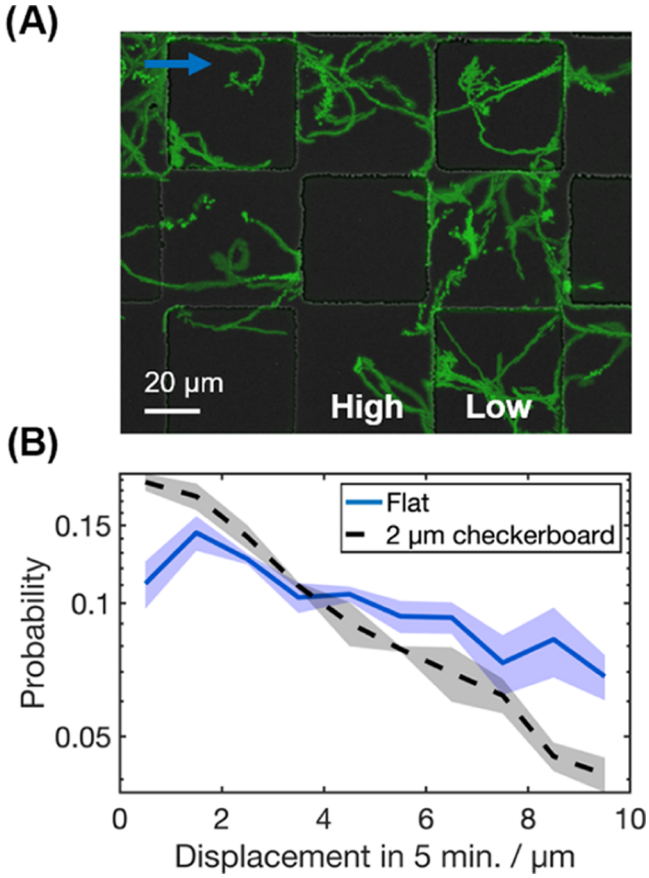

Figure 8. (A) Maximum intensity image of a *P. aeruginosa* time-lapse motility experiment on 2 μm tall checkerboard patterns over the course of 2 h. The fluorescence image of the bacteria (green) is overlaid with a brightfield image of the checkerboard (gray). The steps are spaced by 50 μm on the checkerboard. The blue arrow indicates the direction of the nutrient flow. Some *P. aeruginosa* trajectories are hindered by the walls, and others run alongside the walls. (B) Probability distribution of the displacement of bacteria in 5 min on a flat (solid blue) and a 2 μm tall checkerboard pattern (dashed black). The average is plotted as a solid line, and the shaded regions indicate the standard error.

± 0.1 versus 6.1 ± 0.6 μm on a flat surface. Figure 8B shows a probability distribution of displacement in 5 min of bacteria on a flat surface and a 2 μm tall checkerboard pattern. Compared to a flat surface, the bacteria on a 2 μm tall checkerboard pattern have more short displacement events and fewer long displacement events. It is reasonable that if the steps were to be even closer together, then there would be an even lower probability of long paths.

Mechanism for Motility Inhibition on Steps. There are to date only a few studies of bacterial motility on micrometer-scale topography; so, we are not yet in a position to prove how topography affects motility, but our results provide some insight. Both the work of Meel et al. (*Neisseria gonorrhoeae* and *Myxococcus xanthus*) on grooves[30] and our work (*P. aeruginosa*) find a threshold where topographical barriers of ~1 μm in height are more difficult to cross. Thus, the critical length scale is similar to the dimensions of the bacterium and the length of pili. Recent work has also shown that nanopillar arrays influence surface motility (*P. aeruginosa*), and the authors hypothesize that the available area for attachment for type IV pili may be important,[32] which is similar to the concepts discussed in ref 31.

DOI: 10.1021/acsbiomaterials.9b00729
ACS Biomater. Sci. Eng. 2019, 5, 6436–6445

Meel et al. state "that grooves provide a larger adhesive area for the bacteria than the ridges, explaining why bacteria remain preferentially within the groove...".[30] In prior work, we showed that the motion of *P. aeruginosa* in our systems was lost for mutants lacking pili.[31] Here, we again hypothesize that an important factor is the availability of attachment sites for the pili. This may include the area available for pili attachment and a path for the pili to reach an attachment site.[31] If the topography in a particular direction is not favorable for pili attachment, then that direction of motion may be disfavored. Since our microscopy cannot resolve the type IV pili interactions, we cannot provide direct evidence of how the pili attach on various topographies; we can only discuss the consistency with the observed motion of the bacterial body. We envision that there may be a conformational space in which type IV pili may explore while trying to attach to a surface. We hypothesize that a bacterium's ability to navigate topography is related to the intersection of this conformational space with the surface (Figure 9).

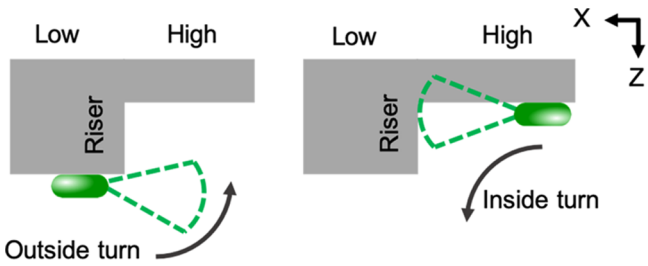

Figure 9. Schematic of the possible available attachment points as *P. aeruginosa* navigates a step. We envision that there is a region of possible conformations that type IV pili may have as they extend (dashed green cone). We hypothesize that the attachment to a surface is less likely when there is minimum intersection of the pilus conformational space with a solid surface, such as for an outside turn (left image). When the bacterium approaches an inside turn (right), the pilus may need less time to find a suitable attachment point on the step, but that attachment may not lead to a crossing.

We propose that when a bacterium crosses a simple step, it must navigate three features: an outside turn, the riser, and an inside turn (see Figure 9). These are the same three features whether the bacterium is going up or down the step. In the limit of a long riser, we assume that the interaction with these three components is independent. Given that the probability of crossing is diminished by the presence of the step (Figure 2), we expect that at least one of these features inhibits the bacterium. When a bacterium approaches an outside turn, it increasingly faces a void ahead, and thus diminishing areas for pilus attachment (see Figure 9, left diagram), which we propose, will inhibit the ability to move forward. A bacterium approaching an inside turn may have a greater area of attachment points for pili due to the presence of the riser (see Figure 9, right diagram) but these attachment points pull the bacterium to the riser, not necessarily over the step. So, both the inside and outside turns could inhibit the crossing. Considering now only those bacteria that do cross, we found that for the long risers (5 and 9 μm), the extra time to cross the step was explained simply by the extra distance to traverse the riser (Figure 5). Somehow, the particular bacteria that do cross do not spend significant extra time to find the appropriate attachment points for their pili for the inside and outside turns. In contrast, for the 3 μm riser, those bacteria that do cross are delayed by the need to turn: they take 2−3× longer than for the equivalent distance on the flat surface. The 3 μm riser is similar in length to the bacterium; so, the three components of the turn cannot be negotiated independently. The combination slows down the bacterium.

Furthermore, we observed some rectification: the bacteria are more likely to cross a high step in the direction against gravity. Rectification requires both asymmetry in the Z direction and some active motion. The active motion is clearly driven by type IV pili. There are several possible sources of asymmetry in our system: the fluid flow, the topography, and the direction relative to gravity. We have shown that the effect of the direction of fluid flow is negligible in our system (see Results and Supporting Information Section 1). The steps were originally etched from top to bottom in silicon; so, in principle, the steps could be asymmetric in this direction, but we could not detect asymmetry in the SEM images. It is also possible that the order of taking the inside and outside turns is the cause of rectification. In our particular setup, the movement across a step in the direction against gravity requires an outside turn followed by an inside turn while the order of turns is reversed for the movement with gravity. So, the rectification may not be due to gravity itself, but due to the different order of crossing the step components. Finally, we explore the possibility that the asymmetry arises from gravity itself. We observed that Δ*fliC* mutants, which lack flagella and therefore are unable to actively swim against gravity, do settle. So, although the force of gravity is insignificant compared to the force of the pilus, the gravitational energy is significant compared to thermal energy (kT). This gravitational force could bias the body to be below the pili on the riser. Because pili-mediated motion is in the direction from the body toward the pili, a body position below the pili would mean a tendency for the bacterium to move in the direction opposing gravity, which is the observed direction of rectification.

CONCLUSIONS

The ability of *P. aeruginosa* to navigate a surface is affected by steps of height greater than 0.4−0.9 μm. Specifically, we find (a) a reduced magnitude of speed perpendicular to the step when the bacteria are very near the step, (b) the probability of crossing the step is drastically reduced compared to crossing a point on a flat surface, and (c) that bacteria are more frequently found near steps, on both the high and low sides. For bacteria that do cross a step, we find a mild rectification of motion against the direction of gravity. Furthermore, there is a time penalty to cross step heights that are similar to the length of the bacterium; however, we do not resolve a time penalty to cross tall steps (5 and 9 μm) in excess of the additional time expected to cross the riser of the step. Images show that *P. aeruginosa* predominantly crawl on the step riser, which means that some bacteria rotate on encountering a step such that the orientation relative to the local topographic plane is similar on the step riser and a flat plane. The bacteria more commonly cross a step where the step is concave relative to the fluid in the $X-Y$ plane. Overall, these findings show that steps with heights similar to the dimensions of the bacteria affect motility. The observed retardation of motion across a plane may be useful for inhibiting colonization and biofilm formation.

ASSOCIATED CONTENT

Supporting Information

The Supporting Information is available free of charge on the ACS Publications website at DOI: 10.1021/acsbiomaterials.9b00729.

DOI: 10.1021/acsbiomaterials.9b00729
ACS Biomater. Sci. Eng. 2019, 5, 6436−6445

Description of methods used to characterize the local radii of curvature of step edges, method of finding the step edge, data on the effects of flow on bacterial motion, figure of average displacement parallel to a step as a function of step height and SEM images of steps (PDF)

AUTHOR INFORMATION

Corresponding Author

*E-mail: wducker@vt.edu.

ORCID

Yow-Ren Chang: 0000-0003-2770-8693

Eric R. Weeks: 0000-0003-1503-3633

William A. Ducker: 0000-0002-8207-768X

Notes

The authors declare no competing financial interest.

ACKNOWLEDGMENTS

The authors thank Prof. Joe Harrison (Univ. of Calgary) for providing the fluorescent strain of *P. aeruginosa*. The authors also thank Prudvi Gaddam (Virginia Tech) and Bob Geil (UNC CHANL) for assistance with the fabrication of the silicon masters used to generate topography, the Fralin Imaging Center (Virginia Tech), the Nanoscale Characterization and Fabrication Laboratory (Virginia Tech), and Chang Lu (Virginia Tech) for the use of equipment and facilities. The authors also thank Prof. Daan Frenkel (Univ. of Cambridge) for useful discussions and for setting up the collaboration. The authors acknowledge financial support from Virginia's 4-VA program and the Institute for Critical Technology and Applied Science (ICTAS) at Virginia Tech for funding and support, and from CAS-TWAS Presidential Scholarship and the National Science Foundation of China (NSFC, Grant 1874398).

REFERENCES

(1) Hall-Stoodley, L.; Costerton, J. W.; Stoodley, P. Bacterial biofilms: from the natural environment to infectious diseases. *Nat. Rev. Microbiol.* **2004**, *2*, 95−108.

(2) Donlan, R. M. Biofilms: microbial life on surfaces. *Emerging Infect. Dis.* **2002**, *8*, No. 95.

(3) Donlan, R. M. Biofilms and device-associated infections. *Emerging Infect. Dis.* **2001**, *7*, 277−281.

(4) Howell, C.; Grinthal, A.; Sunny, S.; Aizenberg, M.; Aizenberg, J. Designing Liquid-Infused Surfaces for Medical Applications: A Review. *Adv. Mater.* **2018**, *30*, No. 1802724.

(5) Epstein, A. K.; Wong, T.-S.; Belisle, R. A.; Boggs, E. M.; Aizenberg, J. Liquid-infused structured surfaces with exceptional anti-biofouling performance. *Proc. Natl. Acad. Sci. USA* **2012**, *109*, 13182−13187.

(6) Ivanova, E. P.; Hasan, J.; Webb, H. K.; Truong, V. K.; Watson, G. S.; Watson, J. A.; Baulin, V. A.; Pogodin, S.; Wang, J. Y.; Tobin, M. J.; et al. Natural bactericidal surfaces: mechanical rupture of *Pseudomonas aeruginosa* cells by cicada wings. *Small* **2012**, *8*, 2489−2494.

(7) Ivanova, E. P.; Hasan, J.; Webb, H. K.; Gervinskas, G.; Juodkazis, S.; Truong, V. K.; Wu, A. H. F.; Lamb, R. N.; Baulin, V. A.; Watson, G. S.; Watson, J. A.; Mainwaring, D. E.; Crawford, R. J. Bactericidal activity of black silicon. *Nat. Commun.* **2013**, *4*, No. 2838.

(8) Gu, H.; Lee, S. W.; Buffington, S. L.; Henderson, J. H.; Ren, D. On-Demand Removal of Bacterial Biofilms via Shape Memory Activation. *ACS Appl. Mater. Interfaces* **2016**, *8*, 21140−21144.

(9) Lee, S. W.; Gu, H.; Kilberg, J. B.; Ren, D. Sensitizing bacterial cells to antibiotics by shape recovery triggered biofilm dispersion. *Acta Biomater.* **2018**, *81*, 93−102.

(10) Levering, V.; Wang, Q.; Shivapooja, P.; Zhao, X.; López, G. P. Soft Robotic Concepts in Catheter Design: an On-Demand Fouling-Release Urinary Catheter. *Adv. Healthcare Mater.* **2014**, *3*, 1588−1596.

(11) Chung, K. K.; Schumacher, J. F.; Sampson, E. M.; Burne, R. A.; Antonelli, P. J.; Brennan, A. B. Impact of engineered surface microtopography on biofilm formation of Staphylococcus aureus. *Biointerphases* **2007**, *2*, 89−94.

(12) Hasan, J.; Chatterjee, K. Recent advances in engineering topography mediated antibacterial surfaces. *Nanoscale* **2015**, *7*, 15568−15575.

(13) Scheuerman, T. R.; Camper, A. K.; Hamilton, M. A. Effects of substratum topography on bacterial adhesion. *J. Colloid Interface Sci.* **1998**, *208*, 23−33.

(14) Kargar, M.; Pruden, A.; Ducker, W. A. Preventing bacterial colonization using colloidal crystals. *J. Mater. Chem. B* **2014**, *2*, 5962−5971.

(15) Kargar, M.; Chang, Y. R.; Hoseinabad, H. K.; Pruden, A.; Ducker, W. A. Colloidal Crystals Delay Formation of Early Stage Bacterial Biofilms. *ACS Biomater. Sci. Eng.* **2016**, *2*, 1039−1048.

(16) Mon, H.; Chang, Y.-R.; Ritter, A. L.; Falkinham, J. O.; Ducker, W. A. Effects of Colloidal Crystals, Antibiotics, and Surface-Bound Antimicrobials on *Pseudomonas aeruginosa* Surface Density. *ACS Biomater. Sci. Eng.* **2018**, *4*, 257−265.

(17) Monds, R. D.; O'Toole, G. A. The developmental model of microbial biofilms: ten years of a paradigm up for review. *Trends Microbiol.* **2009**, *17*, 73−87.

(18) Decker, J. T.; Kirschner, C. M.; Long, C. J.; Finlay, J. A.; Callow, M. E.; Callow, J. A.; Brennan, A. B. Engineered antifouling microtopographies: an energetic model that predicts cell attachment. *Langmuir* **2013**, *29*, 13023−13030.

(19) Ye, Z.; Kim, A.; Mottley, C. Y.; Ellis, M. W.; Wall, C.; Esker, A. R.; Nain, A. S.; Behkam, B. Design of Nanofiber Coatings for Mitigation of Microbial Adhesion: Modeling and Application to Medical Catheters. *ACS Appl. Mater. Interfaces* **2018**, *10*, 15477−15486.

(20) O'Toole, G. A.; Kolter, R. Flagellar and twitching motility are necessary for *Pseudomonas aeruginosa* biofilm development. *Mol. Microbiol.* **1998**, *30*, 295−304.

(21) Klausen, M.; Aaes-Jorgensen, A.; Molin, S.; Tolker-Nielsen, T. Involvement of bacterial migration in the development of complex multicellular structures in *Pseudomonas aeruginosa* biofilms. *Mol. Microbiol.* **2003**, *50*, 61−8.

(22) Skerker, J. M.; Berg, H. C. Direct observation of extension and retraction of type IV pili. *Proc. Natl. Acad. Sci. USA* **2001**, *98*, 6901−4.

(23) Merz, A. J.; So, M.; Sheetz, M. P. Pilus retraction powers bacterial twitching motility. *Nature* **2000**, *407*, 98.

(24) Brill-Karniely, Y.; Jin, F.; Wong, G. C.; Frenkel, D.; Dobnikar, J. Emergence of complex behavior in pili-based motility in early stages of *P. aeruginosa* surface adaptation. *Sci. Rep.* **2017**, *7*, No. 98.

(25) Jin, F.; Conrad, J. C.; Gibiansky, M. L.; Wong, G. C. Bacteria use type-IV pili to slingshot on surfaces. *Proc. Natl. Acad. Sci. USA* **2011**, *108*, 12617−12622.

(26) Conrad, J. C.; Gibiansky, M. L.; Jin, F.; Gordon, V. D.; Motto, D. A.; Mathewson, M. A.; Stopka, W. G.; Zelasko, D. C.; Shrout, J. D.; Wong, G. C. L. Flagella and Pili-Mediated Near-Surface Single-Cell Motility Mechanisms in *P. aeruginosa*. *Biophys. J.* **2011**, *100*, 1608−1616.

(27) Shen, Y.; Siryaporn, A.; Lecuyer, S.; Gitai, Z.; Stone, H. A. Flow directs surface-attached bacteria to twitch upstream. *Biophys. J.* **2012**, *103*, 146−151.

(28) Lecuyer, S.; Rusconi, R.; Shen, Y.; Forsyth, A.; Vlamakis, H.; Kolter, R.; Stone, H. A. Shear stress increases the residence time of adhesion of *Pseudomonas aeruginosa*. *Biophys. J.* **2011**, *100*, 341−350.

(29) Persat, A.; Inclan, Y. F.; Engel, J. N.; Stone, H. A.; Gitai, Z. Type IV pili mechanochemically regulate virulence factors in *Pseudomonas aeruginosa*. *Proc. Natl. Acad. Sci. USA* **2015**, *112*, 7563−7568.

(30) Meel, C.; Kouzel, N.; Oldewurtel, E. R.; Maier, B. Three-Dimensional Obstacles for Bacterial Surface Motility. *Small* **2012**, *8*, 530−534.

(31) Chang, Y.-R.; Weeks, E. R.; Ducker, W. A. Surface Topography Hinders Bacterial Surface Motility. *ACS Appl. Mater. Interfaces* **2018**, *10*, 9225−9234.

DOI: 10.1021/acsbiomaterials.9b00729
ACS Biomater. Sci. Eng. 2019, 5, 6436−6445

(32) Rosenzweig, R.; Perinbam, K.; Ly, V. K.; Ahrar, S.; Siryaporn, A.; Yee, A. F. Nanopillared Surfaces Disrupt *Pseudomonas aeruginosa* Mechanoresponsive Upstream Motility. *ACS Appl. Mater. Interfaces* **2019**, *11*, 10532−10539.
(33) Reddy, S. T.; Chung, K. K.; McDaniel, C. J.; Darouiche, R. O.; Landman, J.; Brennan, A. B. Micropatterned Surfaces for Reducing the Risk of Catheter-Associated Urinary Tract Infection: An In Vitro Study on the Effect of Sharklet Micropatterned Surfaces to Inhibit Bacterial Colonization and Migration of Uropathogenic Escherichia coli. *J. Endourol.* **2011**, *25*, 1547−1552.
(34) Shannon, R. P.; Frndak, D.; Grunden, N.; Lloyd, J. C.; Herbert, C.; Patel, B.; Cummins, D.; Shannon, A. H.; O'Neill, P. H.; Spear, S. J. Using real-time problem solving to eliminate central line infections. *Jt. Comm. J. Qual. Patient Saf.* **2006**, *32*, 479−487.
(35) Sengupta, A.; Lehmann, C.; Diener-West, M.; Perl, T. M.; Milstone, A. M. Catheter duration and risk of CLA-BSI in neonates with PICCs. *Pediatrics* **2010**, *125*, 648−653.
(36) Gottlieb, K.; Mobarhan, S. microbiology of the gastrostomy tube. *J. Am. Coll. Nutr.* **1994**, *13*, 311−313.
(37) Rolston, K. V.; Mihu, C.; Tarrand, J. J. Current microbiology of percutaneous endoscopic gastrostomy tube (PEG tube) insertion site infections in patients with cancer. *Support. Care Cancer* **2011**, *19*, 1267−1271.
(38) Touhami, A.; Jericho, M. H.; Boyd, J. M.; Beveridge, T. J. Nanoscale characterization and determination of adhesion forces of *Pseudomonas aeruginosa* Pili by using atomic force microscopy. *J. Bacteriol.* **2006**, *188*, 370−377.
(39) Crocker, J. C.; Grier, D. G. Methods of digital video microscopy for colloidal studies. *J. Colloid Interface Sci.* **1996**, *179*, 298−310.
(40) Hochbaum, A. I.; Aizenberg, J. Bacteria Pattern Spontaneously on Periodic Nanostructure Arrays. *Nano Lett.* **2010**, *10*, 3717−3721.
(41) Kargar, M.; Wang, J.; Nain, A. S.; Behkam, B. Controlling bacterial adhesion to surfaces using topographical cues: a study of the interaction of *Pseudomonas aeruginosa* with nanofiber-textured surfaces. *Soft Matter* **2012**, *8*, 10254−10259.
(42) Conrad, J. C. Physics of bacterial near-surface motility using flagella and type IV pili: implications for biofilm formation. *Res. Microbiol.* **2012**, *163*, 619−629.

DOI: 10.1021/acsbiomaterials.9b00729
ACS Biomater. Sci. Eng. 2019, 5, 6436−6445